Glass and silicon probes

Castiaux, A.; Danzebrink, H. U.; Bouju, X.

Published in:
Journal of Applied Physics

DOI:
10.1063/1.368095

Publication date:
1998

Document Version
Publisher's PDF, also known as Version of record

Glass and silicon probes: A comparative theoretical study for near-field optical microscopy

A. Castiaux,[a)]
Laboratoire de Physique du Solide, Fac. Univ. Notre-Dame de la Paix, 61, Rue de Bruxelles, B-5000 Namur, Belgium

H. U. Danzebrink
Physikalisch-Technische Bundesanstalt, Bundesallee 100, D-38116 Braunschweig, Germany

X. Bouju
Laboratoire de Physique Moléculaire, U.M.R. C.N.R.S. 6624, Université de Franche-Comté, F-25030 Besançon Cedex, France

(Received 12 December 1997; accepted for publication 26 March 1998)

Glass fibers, chemically etched at their extremities and covered with a thin metal coating, are often present in near-field optical microscopy. Such elongated systems can be used to either probe the evanescent components of the electromagnetic field at the surface of a sample, or locally couple this sample with optical evanescent waves. In this article, we analyze theoretically an alternative tip design made with a silicon core. This kind of probe could be very useful when infrared properties of a surface are to be investigated. The advantages of using such a material for near-field optical detection will be stressed and compared with the performances of a bulk glass fiber. © *1998 American Institute of Physics.* [S0021-8979(98)02513-4]

I. INTRODUCTION

A significant part of the improvements realized for ten years in near-field optical instrumentation is due to the constant evolution of the design of probes used to detect near-field features at the surface of a sample. This element — key piece of all near-field instrumentation — establishes the bond between the experimentalist and the near-field optical phenomena to be observed. From the hole inside a metal screen[1] to the silicon nitride tetragonal tip[2] or the tetrahedral coated tip,[3] a lot of geometries and compositions were investigated in order to build the best probe and to increase the resolution factor. This factor lies on a compromise between two crucial requirements, i.e., the detected intensity and the light confinement resulting from the tip-sample coupling. On one hand, one has to be able to measure weak field intensities, on the other hand, this detection must be as localized as possible. Most of near-field microscopes are now equipped with glass fibers that were elongated and etched at their extremity to obtain a very small scattering center at the apex. For a still better localization of the interaction zone, these glass fibers are often covered with a metallic coating, except a hole at the extremity.

The fabrication process of tips can lead to various shapes, more or less reproducible. Roughly, the extremity of the probe has a conical shape with a paraboloid apex. Always for a confinement concern, very acute conical angles were investigated. However, such ''pin'' tips present an inconvenience. In emission as well as in detection, the light wave traveling inside the tip is early faced with the waveguide cut-off frequency of the fiber, since its section is rapidly decreasing. This problem is even more important when the fiber is coated with metal because the boundary conditions are more drastic: the field has to fall to zero on the surface limiting the tip. For visible wavelength, it is possible to tackle the problem by using probes with a larger opening angle. Since the effective wavelength inside the probe is not large, the propagation inside the very tip is possible. However, when higher wavelengths in the infrared spectrum are considered, usual tips cannot support electromagnetic modes far enough inside the tip, so that they are unusable in emission as well as in detection. It is of prime importance to solve this problem and to find probe configurations that furnish a high resolution also in the infrared range,[4] because near-field infrared features meet more and more interest among the experimentalists.[5,6] The developments of near-field spectroscopy[7–9] promise to obtain a better insight in infrared properties of high importance, especially in the studies of vibrational surface properties, or, more widely, of biological or medical applications.

Our purpose here is to highlight that a silicon tip presents favorable properties to probe near-field phenomena in the infrared range. By comparing the illumination and collection efficiencies of glass and silicon probes in the near-infrared range, we will show the advantages of these new silicon probes.

II. NUMERICAL METHOD AND MODEL

We are faced with a macroscopic light-matter coupling problem where matter is defined by nontrivial boundaries and various dielectric constants. Different methods were already implemented to solve Maxwell's equations as precisely as possible in such complicated geometries.[10–13] One of them, based on Green's propagators, is particularly suited

[a)]Electronic mail: annick.castiaux@fundp.ac.be

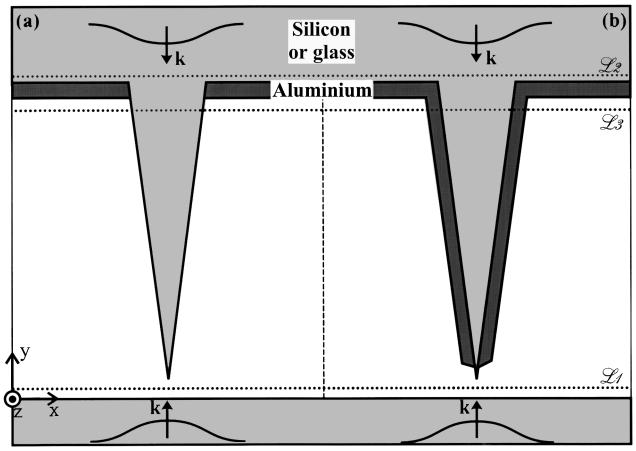

FIG. 1. Model: a Gaussian wave is incident from the top (emitting tip) or the bottom (collecting tip) on a (a) purely dielectric or (b) metallized sharp tip.

to the study of near-field optics problems, where the interactions are localized in a given spatial region.[14]

A. Using Green dyadics to propagate the field

The first stage of this method is a discretization procedure of the material domains $\mathcal{P}$ involved in the interaction. Once this is done, the electromagnetic field is calculated at each discretization cell by solving the following self-consistent Lippmann–Schwinger equation thanks to an original algorithm[15,16]:

$$\mathbf{E}(\mathbf{r},\omega)=\mathbf{E}_0(\mathbf{r},\omega)+\int_{\mathcal{P}} d\mathbf{r}'\,\mathbf{G}_0(\mathbf{r},\mathbf{r}',\omega)\mathbf{V}(\mathbf{r}',\omega)\mathbf{E}(\mathbf{r}',\omega). \tag{1}$$

Here, $\mathbf{E}_0(\mathbf{r},\omega)$ is the unperturbed electric field due to the incident electromagnetic wave and $\mathbf{E}(\mathbf{r},\omega)$ is the total electric field resulting from the light-matter interaction. The field at each perturbation cell is balanced by a potential $\mathbf{V}(\mathbf{r},\omega)$ that depends on the dielectric function at the considered cell. The same kind of equation can also be obtained for the magnetic field $\mathbf{H}(\mathbf{r},\omega)$. Once we know the field in each discretization cell, we can propagate it to any point $\mathbf{r}'$ of the reference medium — the medium embedding the discretized regions — by considering each cell as a pointlike dipole. A Lippmann–Schwinger equation is once more requested to realize this propagation stage, this time without any problem of self-consistency. It is possible to know the electromagnetic field everywhere in the space, without any approximation excepting the acuteness of the discretization procedure.

B. Our model

To compare the efficiency of glass and silicon tips in the near-infrared range, for an incident wavelength $\lambda_0 = 1.3\ \mu$m, we choose a two-dimensional model as the one presented on Fig. 1. Inside the air junction between two semi-infinite dielectric media, we put a very sharp dielectric excrescence on one of the semi-infinite space and facing the other one, to mimic a tip facing a sample. This excrescence is triangular, with an apex angle of 15° and a length of about 2 μm.

The dielectric media are glass ($\epsilon = 2.25$) or undoped silicon ($\epsilon = 12.25$), following the case that we want to investigate. Another parameter is also taken into account: the presence or the absence of a metallic coating along the lateral borders of the tip. This coating is made of aluminum ($\epsilon = -172.73 + i\,32.47$). The (a) and (b) parts of Fig. 1 respectively present the uncoated and coated models. Let us note that small metal screens are also included in the uncoated model. These screens surround the base of the dielectric excrescence in order to enhance the guiding process from or to this tip.

The incident light is simulated by a Gaussian wave (FWHM $= 4\ \mu$m). If we want to consider a collecting tip, this wave is incident from the lower semi-infinite medium. On the contrary, for an emitting tip, it comes from the upper semi-infinite medium.

A particularity of this computation is that the reference medium is not vacuum (nor air), but the dielectric material which the tip and both semi-infinite media are made of. This considerably reduces the importance of the discretized region, that is, the air window and the metal screens. We can thus use a smaller discretization square mesh of 25 nm side. Moreover, since the tip support and the ''sample'' are semi-infinite, we avoid the reflections on the interfaces that usually delimit the back of the tip or the sample. This makes the interpretation of the results easier.

The corrugated profile of the tip due to the discretization procedure could induce an artificial scattering. This can be avoided by considering that the square elements delimiting the probe are truncated by the line of the ideal profile and that the corresponding elements are weighted by the section of the partial area.[17] Such an improvement could allow a better description of the electric field at the edges of the tip. In the present work, we focus on the behavior of the field in the neighborhood of the probe extremity and we choose to keep the profile as designed by the discretization.

III. RESULTS

Using the simulation method explained before, we obtain the distribution of the total electric field intensity $|\mathbf{E}(\mathbf{r},\omega)|^2$ in the computation window described in Fig. 1, for a dielectric tip as well as for a metallized tip. Both emission and detection configurations are considered. Since we choose a two-dimensional model, we have to take into account the two fundamental polarizations, i.e., *s*-polarization, corresponding to an electric field along the translational invariance direction (z-axis), and *p*-polarization, where the incident electric field follows the x-axis (i.e., parallel to the plane of the image). The propagation direction is along the y-axis.

A. *s*-polarization

For this polarization, the light-matter problem can be resumed to a purely scalar calculation. As a matter of fact, the electric field $\mathbf{E}(\mathbf{r},\omega)$ keeps its polarization constant and is completely described by its modulus and phase.

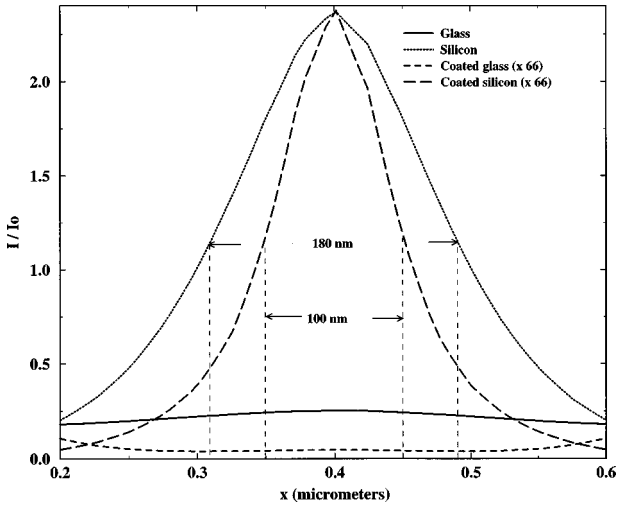

FIG. 2. Emission efficiency for glass and silicon tips, with and without an aluminum coating. For the metallized tips, the emission curves are amplified by a factor 66.

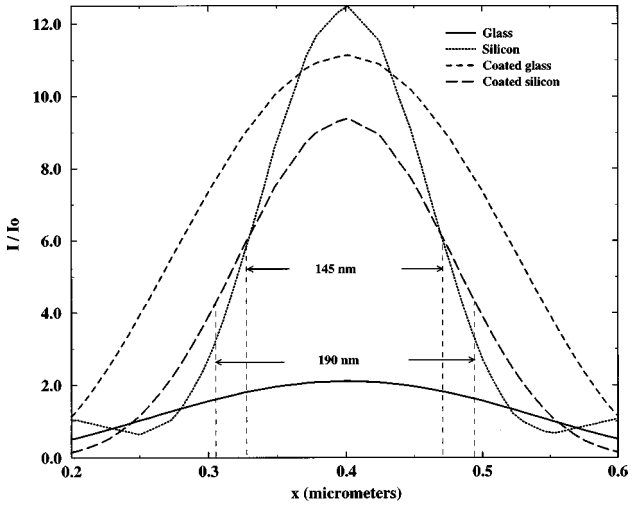

FIG. 3. Penetration intensity for emitting glass and silicon tips, with and without an aluminum coating.

First, let us consider that the tip is used as an illumination source. The incident wave comes from the upper semi-infinite dielectric medium on the tip apex. Since the efficiency of an emitting tip depends on the confinement and the intensity of the spot that it produces,[18] we compute the intensity of the electric field on a line parallel to the x-axis and located just at the apex of the tip (line $\mathcal{L}1$ on Fig. 1). The curves on Fig. 2 allow a comparison between the four considered tips (uncoated or coated glass or silicon tips). With uncoated tips, the total electric field along line $\mathcal{L}1$ presents a maximum. This maximum is about 10 times larger for the silicon tip than for the glass one, due to the transparency of silicon at this infrared wavelength. The curves obtained with coated tips (dashed and long dashed curves, respectively, for glass and silicon cores) are amplified by a factor 66 in order to make the comparison easier. As a matter of fact, the metallization makes the penetration of light inside the tip more difficult since the boundary conditions are more severe. The electric field must vanish at these limiting metallic surfaces and cannot extend outside, contrary to a purely dielectric tip. The spreading of light outside the dielectric tip depends on the constraint imposed on the incident wave by the narrowness of the tip. We can assimilate our tip to a succession of infinitesimal planar waveguides. To each of these local waveguides, i.e., to each y-coordinate of the tip, a cut-off wave number k_c is associated, that becomes larger and larger as the tip narrows. When the wave vector modulus inside the guide is smaller than this k_c, its component in the propagation direction y becomes imaginary and the propagation is no more allowed. This happens for a given y_c level, under which the waves inside the guide are evanescent. For a dielectric tip, light will still propagate by spreading outside the tip. However, when the tip is metallized, this spreading is not possible any more and only evanescent waves will remain in the lower part of the tip.

For the coated glass tip, this vanishing of propagating waves appears too far from the aperture, and no light is emitted by the tip, as it is shown by the dashed curve on Fig. 2. On the contrary, the coated silicon tip allows a penetration of propagating waves almost down to the aperture, and the amount of emitted light is still significant. The principle is the same as the solid lens used in classical microscopy: by increasing the refraction index n of the medium, the resolution is improved. Moreover, the coating concentrates the electric field below the tip apex, what is demonstrated by the diminution of the FWHM (180 and 100 nm for the uncoated and coated silicon tips, respectively).

Let us consider now if the presence of an elongated tip has a positive effect on light confinement or if a simple hole in a metal screen — as the one we have at the base of the tip — would be so efficient. For this purpose, we present four more curves on Fig. 3 that will be compared with the previous ones. These new curves describe the intensity of the electric field along line $\mathcal{L}3$, once the wave begins its way inside the tip, i.e., the distribution of the field as if we had a hole in a metal screen. The first effect of the tip is a considerable intensity loss. This is particularly true for the coated glass probe (dashed curves): while the wave penetrating the tip presents a relatively high intensity, it is almost vanishing at the exit of the tip, for the reasons explained before. The tip acts also on the confinement of the incoming wave. For the dielectric probes (glass or silicon), the exit field is less confined than the incoming one. The wave inclines to scatter outside the tip when it is submitted to a too high constraint by the boundaries of the tip. On the contrary, the confinement is improved through the metallized silicon tip. In this case, the tip canalizes the incoming wave, forcing it to stay on the inside and to acquire a better confinement. Finally, as already said, the coated glass tip has a dramatic effect, since the exit intensity is almost zero.

A last remark about the emission curves of Fig. 2 concerns the nonvanishing background intensity outside the tip-sample interaction zone. For dielectric tips, it is clearly due to the light spreading outside the tip, as we explained before. For coated tips, two phenomena can contribute to the illumination of a larger surface portion. First, the metallization may be too thin and part of the incoming light could escape

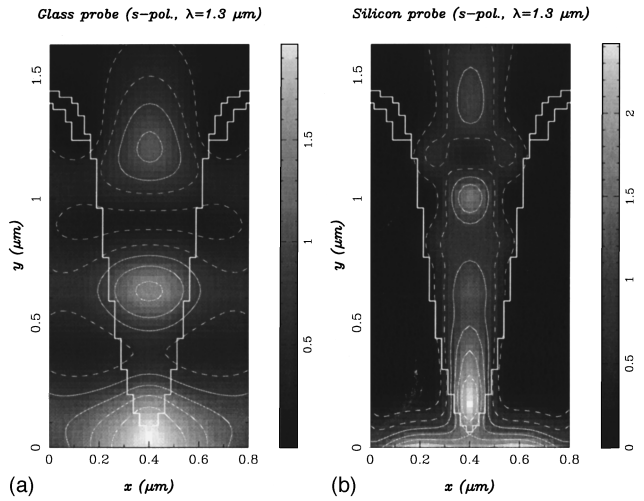

FIG. 4. Distribution of the electric field intensity for dielectric detecting (a) glass and (b) silicon probes.

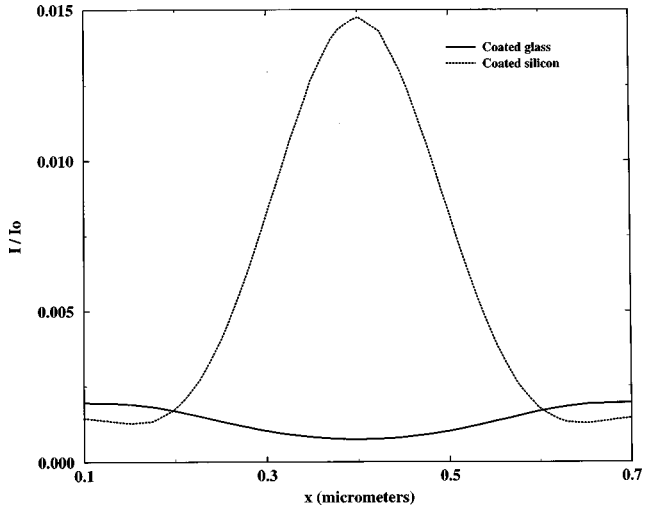

FIG. 5. Detection efficiency inside a glass or a silicon probe coated with aluminum.

from the tip. However, this contribution must be very weak because aluminum has a low skin depth ($\delta \sim 50$ nm for $\lambda = 1.3\ \mu$m). We would rather indict a diffraction effect from the upper metal screens that do not extend beyond the computation window presented on Fig. 1. The incident wave skirts round the external limits of these screens, and adds its contribution to the illumination of the surface. This is a far-field effect.

When the tip is used to detect near fields, the same conditions of confinement and intensity are requested for the tip-sample interaction. The computation of the fields in the near-field zone shows clearly that the confinement request is not fulfilled at all with an uncoated glass probe. On the other hand, a better confinement is obtained with an uncoated silicon probe. This comparison is illustrated on the gray-scale maps given on Fig. 4. A Gaussian wave arriving from the sample on the glass probe interacts just a little with it, and continues its propagation up to the slit between the two small metal screens. When arriving on a silicon tip, the phenomenon is stronger and the light is guided in the probe. However, the interaction area is clearly around 250 to 300 nm. Even if it is well better than with the glass probe, we do not obtain near-field superresolution with our dielectric probe. Dielectric probes seem to need *a priori* high localization of the illumination zone to be effective. As it is mentioned before, dielectric silicon tips are more interesting as illumination sources.

An improvement of the confinement can be again obtained by coating the boundaries of the tip with metallic screens. An incident wave impinging this probe meets a small aperture and tries to penetrate inside the probe through it. Here the confinement is roughly limited by the size of the aperture and thus very good. The problem lies in the difficulty to detect sufficiently high intensities in the near-field zone. Since the effective wavelength of the incident wave is smaller in silicon than in glass, the penetration process is easier, and one can hope to detect a larger amount of light with a silicon tip than with a glass one. In order to put that in evidence, we compute the intensity of the electric field in the detection zone, where the information is transmitted to the observer. The computation zone is drawn as line $\mathcal{L}2$ on Fig. 1 and the intensity of the field along this line for both glass and silicon coated probes is plotted on Fig. 5. The continuous curve, corresponding to the glass probe, is vanishing in the center whereas a small intensity is present on the borders of the computation window. No light is coming from the tip itself, i.e., from the near-field interaction zone, while the incident wave skirts round the small screens to contribute to the lateral intensities. On the contrary, the dotted curve, due to the silicon probe, presents a small but appreciable central intensity, coming right from the near-field coupling zone by means of the probe. In the detection mode, a coated silicon probe should be more efficient in the infrared range.

B. Extrapolation to three-dimensional interpretations

From the preceding study, we can infer some behaviors of the three-dimensional case, close to an experimental context. The two-dimensional computations show that the propagation of light inside the probe is submitted to cut-off conditions. Since the present probes can be considered as a succession of infinitesimal waveguides, the comparison between the cut-off wave numbers k_c of ideal metallized waveguides (see Fig. 6) will help us to draw general conclusions from the two-dimensional study. The first column is

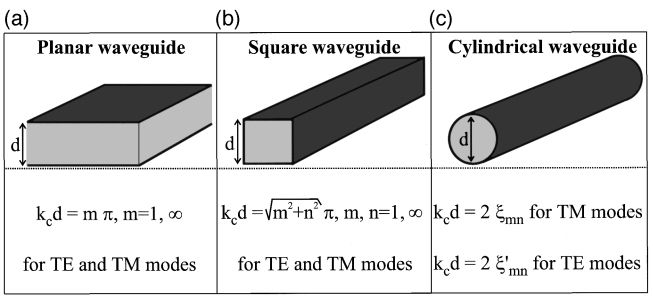

FIG. 6. Cut−off wave numbers for (a) a planar metallized waveguide, (b) a square metallized waveguide, and (c) a cylindrical metallized waveguide.

dedicated to a planar waveguide, the basis of our two-dimensional model. Its thickness is d and the borders are perfect metal plates. The second column concerns a square waveguide, of side d. The last column is for a cylindrical waveguide, which can be related to three-dimensional probes. Its diameter is d. ξ_{mn} and ξ'_{mn} are the nth zeros of, respectively, the cylindrical Bessel function J_m and its derivative J'_m. All these cut-off wave numbers are easily found by using the boundary conditions.[19] If we look at the smallest $k_c d$ value, associated with the first mode, we obtain $k_c d = \pi$ for modes TE_1 and TM_1 in the planar waveguide, as well as for modes TE_{01} and TM_{01} in the square waveguide. For the cylindrical geometry, the first mode is mode TE_{11}, for which $k_c d = 2\xi'_{11} = 3.6$. Thus the study of the two-dimensional geometry gives a rather optimistic point of view, since the cut-off conditions in three-dimensional guides are more severe. Propagation will even be forbidden with larger diameters tips and the decay of evanescent waves will be more fast. So we can extrapolate our conclusions to the three-dimensional case: for near-infrared wavelengths, a silicon probe will be highly more interesting than a glass probe, because the wave vector modulus $k = 2\pi n/\lambda_0$, depending on the index n, is easily larger than k_c.

In order to be complete, we must note that the coatings are not made of perfect metals and are not perfectly flat. On one hand, real metals will lead to a skin effect: light will penetrate inside the metal layer on a small fraction of the wavelength and wall losses will occur, reducing the total intensity of the propagating beam. Since we use experimental dielectric functions[20] to describe the metallic zones in our model, this effect is included in our preceding computations. On the other hand, surface roughnesses will act as scattering centers, producing local enhancements of field intensity. This happens only when there are field components normal to the surface. In a three-dimensional tip, this is always the case. Our preceding computations do not show such surface enhancement, because the s-polarized field is always parallel to the dielectric-metal interfaces. The only way to take this effect into account in our two-dimensional simulations is to consider a p-polarized incident wave. Two illustrations, presented on Fig. 7, compare the detection process with coated probes that are respectively made of glass and silicon. Obviously, a few light penetrates inside the glass probe, whereas the major part of the incident wave skirts round the tip. The intensity level around the tip is saturated to the maximal value that we imposed to align the scales of both computations. On the contrary, the coupling with the silicon probe is efficient: most part of the incident light penetrates inside the tip. The local excitations on the metal boundaries are present in both illustrations. For the glass probe, the external surface shows enhancements of the field where the incident wave meets roughnesses. The same kind of excitations are present inside the silicon probe, since the incident wave penetrates it and is more intense on this inner interface. These illustrations indicate that silicon probes, once more, could be more efficient than glass probes in the detection process. Identical comparisons can be done in p-polarization for the emission case.

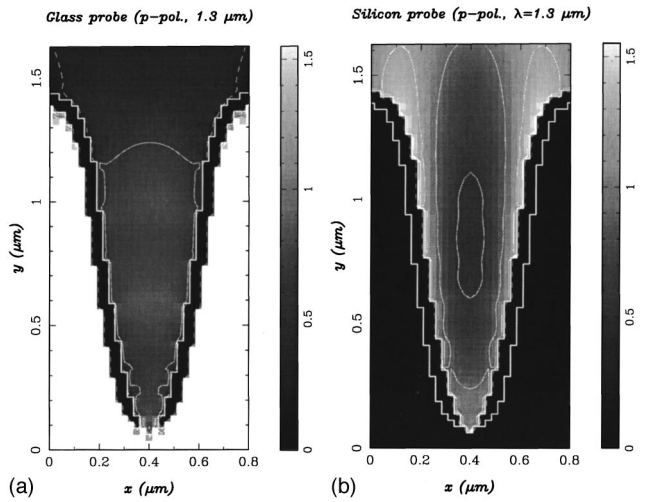

FIG. 7. Distribution of the electric field intensity in the near–field zone, when a coated (a) glass or (b) silicon probe is detecting a Gaussian incident wave.

IV. CONCLUSIONS

Thanks to a two-dimensional model, we highlight the efficiency of silicon probes when they are used to study near-field features in the near-infrared range. A comparison with usual glass probes indicate clearly the advantages of silicon probes as an illumination as well as a detection tool. Especially, aluminum coated silicon probes show a possible resolution around 100 nm, i.e., less than $\lambda/13$.

Since our model is two-dimensional, reservations must be made in respect of quantitative conclusions. However, in order to be able to generalize our qualitative analysis to a three-dimensional reality, we study both s- and p-polarizations. The interest of silicon as probe material is obvious in both cases. We also demonstrate that the use of silicon probes could even be more interesting when three-dimensional probes are involved, since the cut-off problem that makes glass probes unuseful in the infrared spectrum is more crucial when the wave must travel in such a three-dimensional probe.

We deliberately chose a very narrow, acute tip, in order to accentuate the cut-off effects. Near-infrared properties were already studied using tapered glass probes[21,22] and the obtained results were still interesting. However, the propagation problems presented in this article can only be more important when the wavelength increases. Alternative methods to probe the near-field must be elaborated to be able to face these problems. Our purpose here was essentially to propose such a solution, particularly suited for the extension of near-field optics to higher wavelengths: high refractive index probe materials.

ACKNOWLEDGMENTS

The authors want to warmly thank Dr. Ch. Girard (University of Toulouse, France), for numerous fruitful discussions. One of the authors (A.C.) is grateful to the Belgian National Foundation for Research (F.N.R.S.) for financial

support. This work was realized as part of the Human Capital and Mobility program of the European Community.

[1] U. Dürig, D. W. Pohl, and F. Rohner, J. Appl. Phys. **59**, 3318 (1986).
[2] N. F. Van Hulst, M. H. P. Moers, and B. Bögler, J. Microsc. **171**, 95 (1993).
[3] J. Koglin, U. C. Fischer, and H. Fuchs, Phys. Rev. B **55**, 7977 (1997).
[4] A. Lahrech, R. Bachelot, P. Gleizes, and A. Boccara, Opt. Lett. **21**, 1315 (1996).
[5] H. U. Danzebrink, A. Castiaux, Ch. Girard, X. Bouju, and G. Wilkening, Ultramicroscopy **71**, 373 (1998).
[6] A. Lahrech, R. Bachelot, P. Gleizes, and A. Boccara, Appl. Phys. Lett. **71**, 575 (1997).
[7] J. K. Trautman, J. J. Macklin, L. E. Brus, and E. Betzig, Nature (London) **369**, 40 (1994).
[8] Y. Toda, M. Kourogi, and M. Ohtsu, Appl. Phys. Lett. **69**, 827 (1996).
[9] A. Richter, G. Behme, M. Süptitz, Ch. Lienau, and T. Elsaesser, Phys. Rev. Lett. **79**, 2145 (1997).
[10] R. Carminati and J.-J. Greffet, Opt. Commun. **116**, 316 (1995).
[11] D. Barchiesi and D. Van Labeke, Ultramicroscopy **57**, 196 (1995).
[12] L. Novotny, D. W. Pohy, and B. Hecht, Opt. Lett. **20**, 970 (1995).
[13] Ch. Girard and A. Dereux, Rep. Prog. Phys. **59**, 657 (1996).
[14] O. J. F. Martin, Ch. Girard, and A. Dereux, Phys. Rev. Lett. **74**, 526 (1995).
[15] O. J. F. Martin, A. Dereux, and Ch. Girard, J. Opt. Soc. Am. A **11**, 1073 (1994).
[16] A. Castiaux, Ch. Girard, A. Dereux O. J. F. Martin, and J.-P. Vigneron, Phys. Rev. E **54**, 5752 (1996).
[17] Ch. Girard and O. J. F. Martin (private communication).
[18] O. J. F. Martin and Ch. Girard, Appl. Phys. Lett. **70**, 705 (1997).
[19] J. A. Kong, *Theory of Electromagnetic Waves* (Wiley, New York, 1975).
[20] E. D. Palik, *Handbook of Optical Constants of Solids* (Academic, San Diego, 1991).
[21] R. S. Decca, H. D. Drew, and K. L. Empson, Appl. Phys. Lett. **70**, 1932 (1997).
[22] W. D. Herzog, M. S. Ünlü, B. B. Goldberg, G. H. Rhodes, and C. Harder, Appl. Phys. Lett. **70**, 688 (1997).